Journal of Molecular Structure 999 (2011) 2–9

Contents lists available at ScienceDirect

Journal of Molecular Structure

journal homepage: www.elsevier.com/locate/molstruc

Density functional theory studies on 2,5-bis(4-hydroxy-3-methoxybenzylidene)-cyclopentanone

H. Saleem [a,*], Akhil R. Krishnan [a], Y. Erdogdu [b], S. Subashchandrabose [a], V. Thanikachalam [c], G. Manikandan [c]

[a] Department of Physics, Annamalai University, Annamalainagar, Chidambaram 608 002, India
[b] Department of Physics, Ahi Evran University, Kirsehir 40100, Turkey
[c] Department of Chemistry, Annamalai University, Annamalainagar, Chidambaram 608 002, India

ARTICLE INFO

Article history:
Received 16 November 2010
Received in revised form 19 February 2011
Accepted 20 February 2011
Available online 24 February 2011

Keywords:
DFT
HOMO
LUMO
Curcumin
NBO
MEP

ABSTRACT

The optimized molecular structure, vibrational frequencies, corresponding vibrational assignments of 2,5-bis(4-hydroxy-3-methoxybenzylidene)cyclopentanone (BHMBC) have been investigated by using density functional theory (B3LYP) methods at 6-311G(d,p) basis set. The energy and oscillator strength calculated by Time Dependent Density Functional Theory (TD-DFT) results almost compliments with experimental findings. Then, gauge-including atomic orbital (GIAO) ^{13}C NMR and ^{1}H NMR chemical shifts calculations of the BHMBC molecule were carried out by using B3LYP functional with 6-311G(d,p) basis sets. The mass spectrum is also recorded. Moreover, we have not only simulated highest occupied molecular orbital (HOMO) and lowest unoccupied molecular orbital (LUMO) but also determined the transition state and energy band gap. The stability of the molecule arising from hyperconjugative interaction and charge delocalization has been analyzed using natural bond orbital (NBO) analysis. Besides, molecular electrostatic potential (MEP) were performed by the DFT method and the infrared and Raman intensities have also been reported.

1. Introduction

The title compound 2,5-bis(4-hydroxy-3-methoxybenzylidene)cyclopentanone (BHMBC) is a curcumin derivative. Curcumins have several biological activities, such as anti-inflammatory, antioxidative, antibacterial, antihepatotoxic, hypertensive and hypocholesterolenic properties [1–5]. Curcumin inhibits *in vitro* lipid peroxide formation by liver homogenates of endemic mice [6]. It is used for the synthesis of bioactive pyrimidine compounds [7] and also find applications in the preparation of liquid–crystalline polymers [8]. Thermo tropic liquid crystalline behavior of polymeric materials containing cyclopentanone moiety linked with polyethylene spacers is of considerable current interest, not only because of their potential as high-strength fibers, plastics, moldings, etc. [9–11], but also their applications in non-linear optical materials [12]. The benzylidene derivatives are intermediates in various pharmaceuticals, agrochemicals and perfumes [13]. Curcumin demonstrated a great ability in chelating essential metal ions such as Cu (II) [14] and the complexes showed a higher scavenging ability than curcumin.

The theoretical study on physicochemical properties of curcumin has been reported [15]. Spectroscopic and theoretical study of the electronic structure of curcumin and related fragment molecules were carried out [16]. Density functional theory investigation of Cu (I) and Cu (II) curcumin complexes were reported [17]. A theoretical study based on comparison of calculated spectroscopic properties with NMR, UV–visible and IR experimental data is done [18]. A combined theoretical and experimental approach to the study of the structure and electronic properties of curcumin as a function of solvent is also reported [19].

Literature reveals that to the best of our knowledge DFT calculations and experimental studies on BHMBC molecule have not been reported so far. Therefore, the present work deals with FT-IR, FT-Raman, Mass spectra, UV and NMR spectroscopic investigation of BHMBC utilizing DFT (B3LYP) method with 6-311G(d,p) as basis set. Vibrational spectrum of the molecule supported by using the Scaled Quantum Mechanical (SQM) force field technique based on density functional theory (DFT). All possible conformers of BHMBC molecule have been optimized at B3LYP levels at 6-311G(d,p) level. The redistribution of electron density (ED) in various bonding and antibonding orbitals and E2 energies have been calculated by natural bond orbital (NBO) analysis using DFT method to give clear evidence of stabilization originating from the hyper conjugation of various intra-molecular interactions. The HOMO and LUMO analysis have been used to elucidate information regarding charge transfer within the molecule.

* Corresponding author. Tel.: +91 9443879295.
E-mail address: saleem_h2001@yahoo.com (H. Saleem).

0022-2860/$ - see front matter © 2011 Elsevier B.V. All rights reserved.
doi:10.1016/j.molstruc.2011.02.039

2. Experimental details

2.1. Preparation of 2,5-bis(4-hydroxy-3-methoxybenzylidene)cyclopentanone

Vanillin (1 mmol) and cyclopentanone (0.5 mmol) were heated in a water bath (45–50 °C) until a clear solution was obtained; concentrated hydrochloric acid was then added followed by 2 h stirring. After standing overnight, the mixture was treated with cold aqueous acetic acid (1:1) and filtered. The solid material was washed first with cold ethanol, then with hot water and dried in a vacuum. The yellow substance was recrystallized from ethanol (m.p. = 212 °C; lit. = 212–214 °C) [20].

2.2. Instruments

The FT-Raman spectrum of BHMBC was recorded using the 1064 nm line of a Nd:YAG laser as excitation wavelength in the region 10–3500 cm^{-1} on a Brucker model IFS 66 V spectrophotometer equipped with an FRA 106 FT-Raman module accessory. The FT-IR spectrum of this compound was recorded in the region 400–4000 cm^{-1} on an IFS 66 V spectrophotometer using the KBr pellet technique. The spectrum was recorded at room temperature, with a scanning speed of 10 cm^{-1} per minute and at the spectral resolution of 2.0 cm^{-1}. The observed experimental FT-IR and FT-Raman spectra along with theoretical spectra of BHMBC are shown in Figs. S1 and S2. The ultraviolet absorption spectrum of BHMBC was examined in the range 200–500 nm using a Shimadzu UV-2401PC, UV–visible recording spectrometer. The UV pattern is taken from a 10^{-5} molar solution of BHMBC dissolved in methanol. ^1H NMR spectrum was measured in $CDCl_3$ and DMSO and ^{13}C NMR is measured in $CDCl_3$ at ambient temperature on a Varian Mercury-VxBB 300 spectrometer (299.95 MHz for ^1H and 75.43 MHz for ^{13}C). The spectral measurements were carried out at Sree Chitra Tirunal Institute for Medical Sciences and Technology, Poojappura, Thiruvananthapuram, Kerala, India. Mass spectrum of BHMBC was recorded in chloroform solvent in Perkin Elmer SCIEX-ATI-3000 model, at Orchid Research Laboratories, Research and Development Center, Chennai, India.

3. Computational details

For meeting the requirements of both accuracy and computing economy, theoretical methods and basis sets should be considered. DFT has proved to be extremely useful in treating electronic structure of molecules. The density functional three parameter hybrid model (DFT/B3LYP) at 6-311G(d,p) basis set level was adopted to calculate the properties of the molecule in this work. All the calculations were performed using the Gaussian 03w program package [21] with the default convergence criteria without any constraint on the geometry [22]. It should be noted that Gaussian 03 package does not calculate the Raman intensities. The Raman activities were transformed into Raman intensities using Raint program [23] by the expression:

$$I_i = 10^{-12}\frac{(v_0 - v_i)^4}{v_i \cdot S} \quad (1)$$

where I_i is the Raman intensity. S is the Raman scattering activities, v_i is the wavenumber of the normal modes and v_0 denotes the wavenumber of the excitation laser [24]. For B3LYP functional, selected as the one which gives the most accurate result, calculations were continued with the expanded 6-311G(d,p) basis set. The results obtained at this level of theory, were used for the detailed interpretation of the infrared and Raman spectra. The total energy distribution (TED) was calculated by using the scaled quantum mechanics (SQM) program [25,26] and the fundamental vibrational modes were characterized by their TED.

4. Results and discussion

4.1. Molecular geometry

All possible conformers of BHMBC molecule have been optimized at B3LYP level at 6-311G(d,p) level are shown in Fig. 1. The optimized energies of conformers are given in the Table 1. The relative energy of the conformers are determined at 0.0 kJ/mol (conformer 3), 20.241 kJ/mol (conformer 2), 23.094 kJ/mol (conformer 1) and 31.759 kJ/mol (conformers 9 and 15) for B3LYP/6-311 G(d,p) level of theory. The optimized energy of other conformers is higher than those of conformer 3. As a result, the energy obtained for conformer 3 of BHMBC molecule was found to be the global minimum.

The most stable conformer of the title compound belongs to C_1 point group symmetry. The optimized molecular structure of BHMBC is shown in Fig. 2. Title molecule contains two hydroxyl and methoxy groups in benzene ring, both the benzene rings are attached to the cyclopentanone ring at C_{21} and C_{22} carbon. Optimized bond lengths, bond angles and dihedral angles of the molecule are predicted using B3LYP/6-311G(d,p) levels and it is mentioned in Table S1.

In the literature, we have found neither experimental data nor calculated results on molecular structure of BHMBC. Therefore, the molecular structure of BHMBC is compared with the available X-ray diffraction data [27]. The most of the optimized bond lengths and bond angles calculated at B3LYP/6-311G(d,p) method correlates well with the experimental values. The bond distance of C_1—C_2 is 1.410 Å at B3LYP/6-311G(d,p) method. The reasoning of larger bond length appears in the bond is repulsive and attractive forces of unlike charges. The maximum bond length has calculated for C_{21}—C_{41} (1.507 Å), C_{22}—C_{42} (1.509 Å) and C_{41}—C_{42} (1.559 Å). This is in agreement with the literature values [27]. Carbonyl group has the bond distance 1.423, 1.356, 1.374 and 1.422 Å (O_{12}—C_{13}, C_{29}—O_{39}, C_{32}—O_{34} and O_{34}—C_{35} respectively). Bond distance of hydroxyl group is measured about 0.967 Å (O_{10}—H_{11}, O_{39}—H_{40}). Optimized bond angle of C_2—C_1—C_6 are 119.3° using B3LYP method respectively. The C_2—C_1—O_{10}, O_{20}—C_{19}—C_{21} bonds have different angles (120.2° and 125.9°) and this is due to the dominant electron density in oxygen than carbon and hydrogen, in other case elongation of pentanone ring is observed. The C—C—H bond angle of the molecule increases and decreases towards 120°. Among the bond angles of O—C—H, O34—C35—H36 bond have minimum angle about 106.0°. The C—C—C bond angles end with hydrogen atom have maximum bond angle in the molecule (C_4—C_{17}—C_{21}: 131.5°, C_{17}—C_{21}—C_{41}: 131.2°, C_{22}—C_{23}—C_{28}: 131.9° and C_{23}—C_{22}—C_{42}: 131.2°). The planarity of the molecule is confirmed by the dihedral angle values from 0° to 180°. Even though there were some differences between the calculated and the literature values, the optimized structure parameters well reproduce the literature values. The small difference between the computed data is due to calculation belongs to gaseous phase and experimental result belong to solid phase.

4.2. Vibrational assignments

Vibrational spectral assignments were performed on the recorded FT-IR and FT-Raman spectra based on the theoretically predicted wavenumbers by density functional B3LYP/6-311G(d,p) method and are collected in Table S2. None of the predicted vibrational spectra has any imaginary wavenumbers, implying that the optimized geometry is located at the local lowest point on the po-

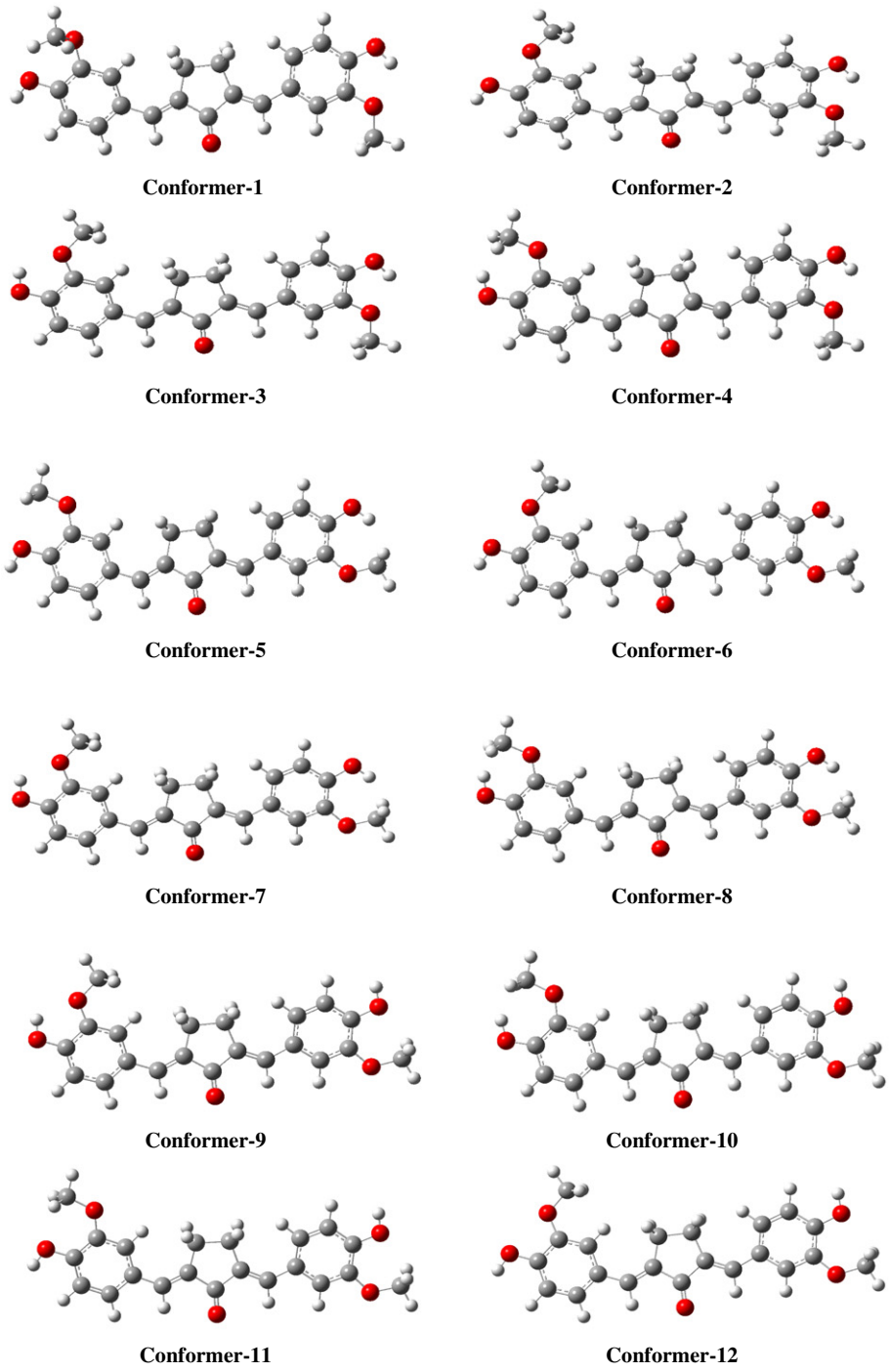

Fig. 1. All possible conformers of BHMBC.

tential energy surface. We know that the DFT potentials systematically overestimate the vibrational wavenumbers. These discrepancies are corrected either by computing anharmonic corrections explicitly or by introducing a scaled field [28] or by directly scaling the calculated wavenumbers with a proper factor [29]. We calibrated the vibrational wavenumbers by using scaling factors of 0.9663 for B3LYP level of theory. After scaling with a scaling factor, the deviation from the experimental value is less than 10 cm^{-1} with a few exceptions. The title molecule belongs to C_1 point group. Comparison of the wavenumbers calculated with experimental values reveal that the B3LYP method shows very good agreement with experimental observation due to inclusion of electron correlation for this method.

4.2.1. O—H vibrations

The O—H group gives rise to three vibrations (stretching, in-plane bending and out-of-plane bending vibrations). The O—H group vibrations are likely to be the most sensitive to the environment, so they show pronounced shifts in the spectra of the hydrogen-bonded species. The hydroxyl stretching vibrations are generally observed in the region around 3500 cm^{-1} [30]. In the case of the unsubstituted phenols, it has been shown that the

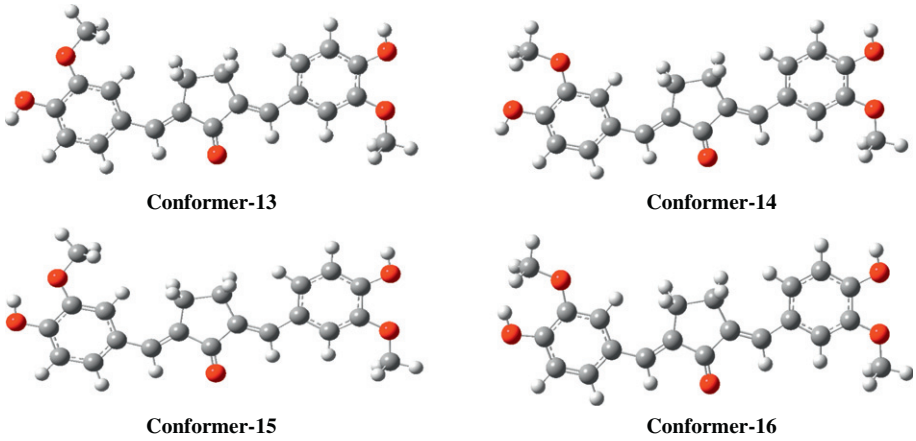

Fig. 1 (*continued*)

Table 1
The optimized energy of all possible conformers of BHMBC.

Conformers	Energy (a.u.)	Relative energy (kJ/mol)
Conformer-1	−1188.66	23.09
Conformer-2	−1188.66	20.24
Conformer-3	−1188.67	0.00
Conformer-4	−1188.65	42.36
Conformer-5	−1188.64	72.95
Conformer-6	−1188.64	64.38
Conformer-7	−1188.65	44.20
Conformer-8	−1188.63	86.57
Conformer-9	−1188.65	31.76
Conformer-10	−1188.64	73.97
Conformer-11	−1188.64	60.25
Conformer-12	−1188.65	51.84
Conformer-13	−1188.65	41.24
Conformer-14	−1188.65	49.68
Conformer-15	−1188.65	31.76
Conformer-16	−1188.64	63.33

wavenumber of O—H stretching vibration in the gas phase is at 3657 cm^{-1} [31]. Similarly, in our case the band at 3640 and 3639 cm^{-1} [mode no's: 132,131] in B3LYP are assigned to O—H stretching vibrations and is evident from the TED column they are almost contributing to100%.

The O—H in-plane bending vibrations for phenols, in general, lies in the region 1150–1250 cm^{-1} and is not much affected due to hydrogen bonding unlike to stretching and out-of-plane bending wavenumbers [32]. In our present study, the O—H in-plane bending vibration computed by B3LYP/6-311G(d,p) method at 1238, 1198 and 1172 cm^{-1} [mode no's: 83, 80, 77] show very good agreement with the recorded FT-Raman band at 1200, 1165 cm^{-1} and 1222, 1169 cm^{-1} in FT-IR, respectively. The O—H out-of-plane deformation vibration for phenol lies in the region 290–320 cm^{-1} for free OH and in the region 517–710 cm^{-1} for associated OH [31]. In both inter-molecular and intra-molecular associations, the wavenumber is at a higher value than in free OH. The O—H out-of-plane bending vibration computed by B3LYP at 472 cm^{-1} [mode no: 32] has a TED contribution of 83%.

4.2.2. C—H vibrations

In the heteroaromatic compounds, the C—H stretching vibrations normally occur at 3100–3000 cm^{-1} [33]. These vibrations are not found to be affected by the nature and position of the substituent and typically exhibit weak bands compared with the aliphatic stretching vibrations. In infrared spectra, most of the aromatic compounds have nearly four peaks in the region 3080–3010 cm^{-1} due to ring C—H stretching bands. IR frequencies of C—H bands are a function of sp hybridization [34]. The scaled vibrations, [mode no's: 130–121, 118–115] assigned to the aromatic C—H stretch computed in the range 3140–3018 cm^{-1} and 2953–2912 cm^{-1} by B3LYP/6-311G(d,p) method shows good agreement with the recorded weak FT-IR band at 2922 cm^{-1}. As

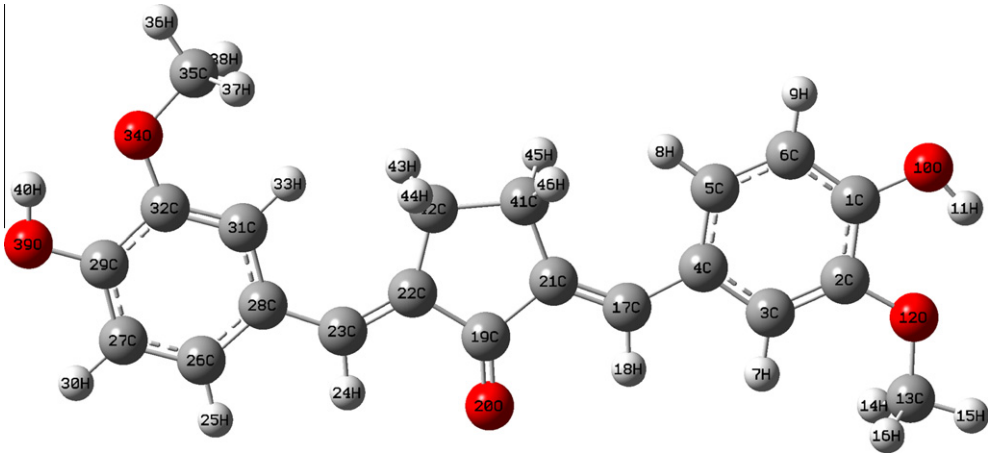

Fig. 2. Optimized structure of BHMBC.

expected, these sixteen modes are pure stretching modes as it is evident from TED column and they are almost contributing to 98%.

The C—H in-plane bending vibrations are usually expected to occur in the region 1300–1000 cm^{-1} and these vibrations are very useful for characterization purposes [34]. Six medium strong peaks at 1367, 1222, 1169, 1122, 1031 and 996 cm^{-1} in FT-IR and seven very weak peaks at 1369, 1317, 1245, 1200, 1165, 1123 and 1096 cm^{-1} in FT-Raman spectrum are assigned to the C—H in-plane-bending vibration. These values are in good agreement with the theoretically computed B3LYP method at 1369, 1288, 1238, 1211, 1158, 1111, 1108, 1025, 987 cm^{-1} [mode no's: 92, 89, 83, 81, 76, 70, 69, 67, 65]. These vibrational modes were observed as mixture of C=C, C—C, C—O vibrations. The C—H out-of-plane bending vibrations are strongly coupled and occur in the region 1000–700 cm^{-1} [35]. Generally, the C—H out-of-plane deformation modes owned the highest wavenumbers have weaker intensity than these observing at lower wavenumbers [36]. In the title molecule BHMBC, the peaks observed at 996, 845 and 793 cm^{-1} in the FT-IR spectrum confirms the C—H out-of-plane bending vibrations. It is good agreement with the theoretically scaled harmonic wavenumber values at 987, 956, 841, 833 and 799 cm^{-1} in B3LYP [mode no's: 65, 62, 56, 55, 52].

4.2.3. C=O vibrations

The carbon–oxygen double bond is formed by pπ–pπ bonding between carbon and oxygen. Because of the different electro negativities of carbon and oxygen atoms, the bonding electrons are not equally distributed between the two atoms [37]. Normally, the carbonyl group vibrations occur in the region 1780–1680 cm^{-1}. In the present study, the experimental wavenumber observed as a weak band at 1669 cm^{-1} in the FT-IR spectrum is assigned to C=O stretching vibration, which is in agreement with the B3LYP method at 1691 cm^{-1} [mode no: 112] with a TED contribution of 61%. The very weak band observed at 1245 cm^{-1} in FT-Raman and strong peak observed at 1222 cm^{-1} in FT-IR is assigned to C—O stretching vibration, which is not only in well agreement with the theoretical values: 1242, 1238, 1223 cm^{-1} [mode nos: 84, 83, 82] at B3LYP but also the literature values [38]. The computed vibrational modes 80, 77, 76 are assigned to C—OH in-plane-bending vibration (1198, 1172, 1158 cm^{-1}) which is in satisfactory agreement with the recorded FT-IR at 1169 cm^{-1} and FT-Raman at 1200, 1165 cm^{-1} also find support from literature [39], the C—OH out-of-plane bending vibration is assigned to mode no's: 29–27, 24 [446, 440, 430, 341 cm^{-1}] in B3LYP method.

4.2.4. CH_3 vibrations

In BHMBC, there are two CH_3 groups attached to the benzene ring and we expect number of stretching and bending vibrations. In aromatic molecules, the asymmetric stretching vibrations of CH_3 are expected to appear in the range of 3000–2905 cm^{-1} and symmetric stretching vibrations are in the range of 2870–2860 cm^{-1} [40,41]. In our study, the vibrational frequencies of 2969, 2966 cm^{-1} [mode no's: 120, 119] calculated by B3LYP are assigned to CH_3 asymmetric stretching and CH_3 symmetric vibration is assigned at 2910, 2907 cm^{-1} [mode no's: 114, 113] by B3LYP method for both methyl groups present in the molecule and it is in good agreement with the experimental value observed at 2922 cm^{-1} in FT-IR. The in-plane bending vibrations (scissoring) of the CH_3 groups have been identified by the B3LYP method at 1457, 1456, 1449 cm^{-1} (mode no's: 103, 102, 101) and the out-of-plane bending vibration (umbrella) at 1440, 1436, 1415 cm^{-1} (mode no's: 99, 97, 95). They show good agreement with the literature values [42]. The CH_3 wagging vibrations computed by B3LYP method at 1211, 1198 cm^{-1} [mode no's: 81, 80] show good agreement with the recorded spectral value observed at 1200 cm^{-1} in FT-Raman.

Table 2
Calculated electronic absorption spectrum of BHMBC.

Excitation	CI expansion coefficient	Wavelength (nm)		Oscillator strength (*f*)
		Calc.	Expt.	
Excited state 1				
91 → 94	0.69	405.64	422.00	0.00
Excited state 2				
93 → 94	0.65	396.53	420.40	1.11
Excited state 3				
92 → 94	0.64	357.14	405.40	0.02
93 → 95	−0.18			

4.2.5. Ring vibrations

The ring carbon–carbon stretching vibrations occur in the region 1625–1430 cm^{-1}. In general, the bands are of variable intensity and are observed at 1625–1575, 1540–1470, 1465–1430 and 1380–1280 cm^{-1} from the wavenumber ranges given by Shimanouchi et al. [43] for five bands in the region. In the present investigation, the wavenumbers observed at 1592 cm^{-1} in FT-Raman and 1577 cm^{-1} in FT-IR have been assigned to C=C stretching vibration. The theoretically computed values by B3LYP at 1612, 1604, 1587, 1576, 1574 cm^{-1} [mode no's: 111, 110, 109, 108, 107] show excellent agreement with experimental values. The aromatic stretching vibrations give rise characteristic bands in both the observed IR and Raman spectra, covering the spectral range from 1600 to 1400 cm^{-1} [44–48]. The observed FT-IR and FT-Raman bands are 1519, 1422, 1560 and 1422 cm^{-1} respectively, among these bands, 1519 and 1560 cm^{-1} are appeared as strong and very strong in nature. The calculated bands at B3LYP level [mode no's: 106, 105, 95] in the same region are in excellent agreement with experimental observations of both in FT-IR and FT-Raman spectra of BHMBC. The C—C in-plane bending vibration calculated at 475 cm^{-1} by B3LYP/6-311G(d,p) method (mode no: 33) is in good agreement with the spectral value observed at 477 cm^{-1} in FT-IR and the C—C out-of-plane bending vibration is assigned to 460, 446, 430 and 353 cm^{-1} [mode no: 30, 29, 27, 26] in B3LYP method. In addition, there are several C—C—C in-plane and out-of-plane bending vibrations of the benzene ring carbons. The theoretically calculated C—C—C in-plane and out-of-plane bending vibrations are in agreement with literature values [49].

5. UV analysis

UV–visible absorption spectrum of BHMBC in diluted methanol solution is given in Fig. S3. Absorption maximum (λ_{max}) of the molecule is calculated by TD-DFT (B3LYP) method. The calculated visible absorption maximum of λ_{max} which is a function of the electron availability has been reported in Table. 2. On the basis of fully optimized ground-state structure, TD-DFT calculations have been used to determine the low-lying excited states of BHMBC. The calculated results involving the vertical excitation energies, oscillator strength (*f*) and wavelength are carried out and compared with measured experimental wavelength. Typically, according to Frank–Condon principle, the maximum absorption peaks (λ_{max}) correspond in a UV–visible spectrum to vertical excitation. From the Table 2, it is evident that the intense electronic transition predicted by TD-DFT//B3LYP/6-311G(d,p) correlates well with the measured experimental values as shown in Fig. S3.

It can be seen from the Fig. S3 that the compound comprises two bands in the wavelength range from 250 to 500 nm. The bands at shorter wavelength (250–280 nm) are due to its localized $*$ transition of the phenyl moieties, while the longer wavelength bands with λ_{max} ranging from 400–430 nm can be assigned to the intra-

Table 3
Theoretical and experimental ^{1}H and ^{13}C spectra of BHMBC (with respect to TMS, all values in *ppm*).

Atoms	Exp.	B3LYP/6-311G(d,p)	Atoms	Exp.	B3LYP/6-311G(d,p)
C_{19}	195.89	196.1	H_{33}	7.52	7.536
C_{29}		154.5	H_{18}		7.510
C_1		154.5	H_{24}	7.31	7.465
C_{32}	148.06	151.9	H_8		7.310
C_2	147.32	151.5	H_{25}		7.250
C_{22}		140.6	H_9		7.079
C_{21}		139.8	H_7	6.97	7.059
C_{17}		138.2	H_{30}	6.98	6.989
C_{23}		137.7	H_{11}		5.799
C_{26}		133.2	H_{37}		5.793
C_{28}	134.66	132.4	H_{40}		4.189
C_4		132.4	H_{15}		4.188
C_{31}		127.3	H_{36}	3.94	3.825
C_5		118.0	H_{16}		3.825
C_{27}		116.9	H_{14}		3.776
C_3		116.5	H_{38}		3.771
C_6	113	112.2	H_{46}		3.111
C_{35}		55.03	H_{43}		3.110
C_{13}	55.77	55.01	H_{44}	2.17	3.008
C_{41}		28.77	H_{45}	2.15	3.008
C_{42}	26.32	28.37			

molecular charge transfer transition involving the whole electronic system of the compound with a considerable charge transfer character originating mainly from the substituted phenyl moiety and pointing towards the carbonyl group. Calculations of molecular orbital geometry show that the visible absorption maximum of this molecule corresponds to the electron transition between frontier orbitals such as translation from HOMO to LUMO.

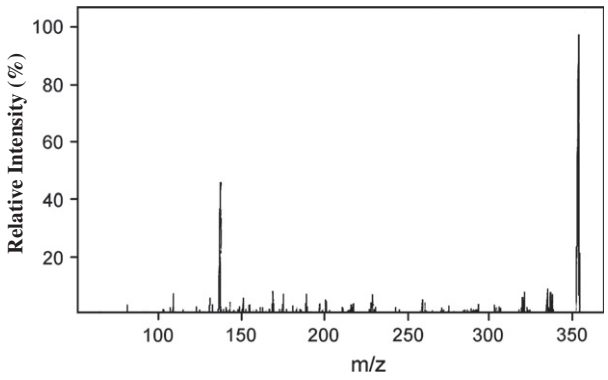

Fig. 4. Mass spectrum of BHMBC.

6. NMR analysis

The molecular structure of the BHMBC molecule was optimized. Then, gauge-including atomic orbital (GIAO) ^{13}CNMR and ^{1}HNMR chemical shift calculations of the BHMBC molecule were carried out by using B3LYP functional with 6-311G(d,p) basis set. The NMR spectra calculations were performed by using the Gaussian 09 [50] program package. The calculations reported were performed in DMSO solution using the IEF-PCM model, rather than in the gas phase, in agreement with experimental chemical shifts obtained in DMSO solution.

The experimental and calculated values for ^{13}C and ^{1}H NMR as shown in Table. 3 correlates well with each other. ^{1}H NMR ($CDCl_3$ and DMSO-d_6 ppm): 7.31 (2H, —OH protons), 6.97–6.98 (2H, aromatic hydrogen), 7.52 (2H, —CH=), 3.94 (6H, OCH_3 protons),

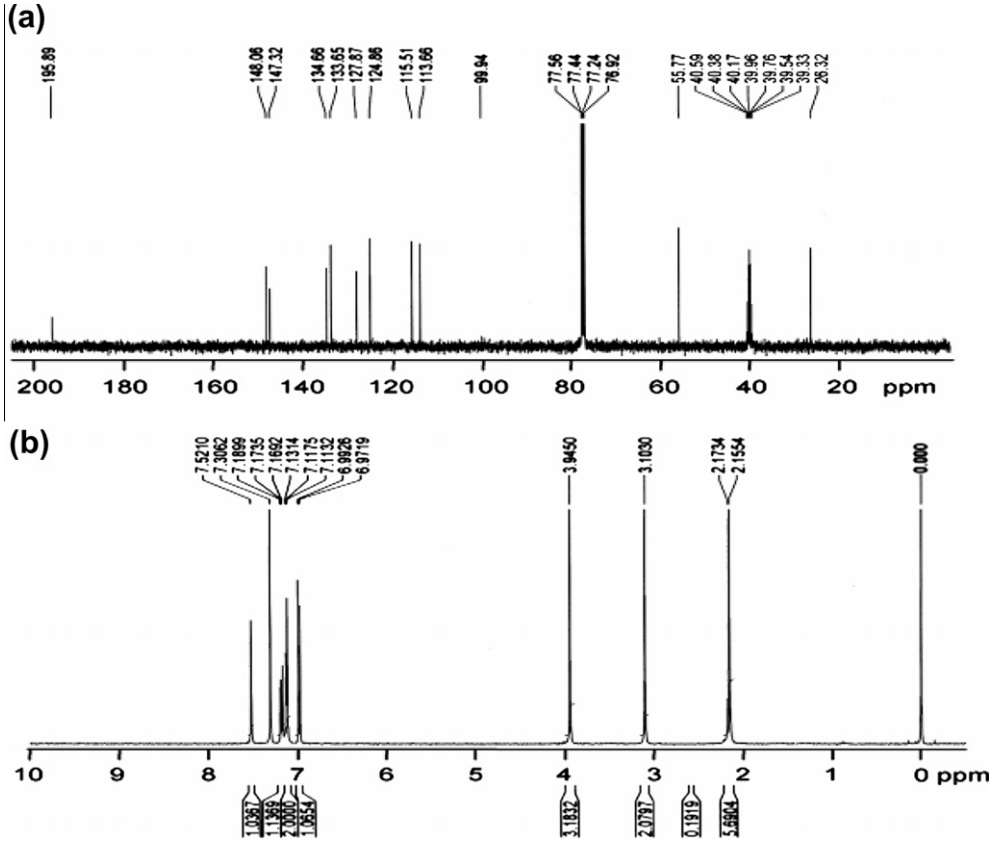

Fig. 3. The observed (a) ^{13}C NMR and (b) ^{1}H NMR of BHMBC.

2.15–2.17 (4H, $-H_2C-CH_2-$). ^{13}C NMR ($CDCl_3$ ppm): 195.89 (C=O), 148.06–147.32 (CH, C=C, C—O), 113–134.66 (aromatic carbons), 55.77 (OCH_3), 26.32 (CH_2). The observed ^{13}C NMR and ^1H NMR of BHMBC is shown in Fig. 3.

7. Mass spectrum

Sample was initially dissolved in $CHCl_3$ and serial dilution was carried out in a positive ionization mode. The m/z range was extended sufficiently to detect the presence of molecular ion peak at m/z = 354 and its relative intensity with respect to the monomer benzylide unit (Fig. 4).

8. NBO analysis

Natural bond orbital analysis gives the accurate possible natural Lewis structure picture of ø because all orbital are mathematically chosen to include the highest possible percentage of the electron density. Interaction between both filled and virtual orbital spaces information is correctly explained by the NBO analysis, it could enhance the analysis of intra- and inter-molecular interactions. The second order Fock matrix was carried out to evaluate donor (i)–acceptor (j) i.e. donor level bonds to acceptor level bonds interaction in the NBO analysis [51]. The result of interaction is a loss of occupancy from the concentration of electron NBO of the idealized Lewis structure into an empty non-Lewis orbital. For each donor (i) and acceptor (j), the stabilization energy $E(2)$ associates with the delocalization $i \rightarrow j$ is estimated as

$$E(2) = -n_\sigma \frac{\langle \sigma | F | \sigma \rangle^2}{\varepsilon_{\sigma^*} - \varepsilon_\sigma} = -n_\sigma \frac{F_{ij}^2}{\Delta E} \quad (2)$$

where q_i is the donor orbital occupancy, $\boldsymbol{\varepsilon}_j$ and $\boldsymbol{\varepsilon}_i$ are diagonal elements and $F(i,j)$ is the off diagonal NBO Fock matrix element. Natural bond orbital analysis provide an efficient method for studying intra and inter-molecular bonding and interaction among bonds, and also provides a convenient basis for investigating charge transfer or conjugative interaction in molecular systems. Some electron donor orbital, acceptor orbital and the interacting stabilization energy resulted from the second-order microdisturbance theory are reported [52,53]. The larger $E(2)$ value the more intensive is the interaction between electron donors and acceptor i.e. the more donation tendency from electron donors to electron acceptors and the greater the extent of conjugation of the whole system [42]. Delocalization of electron density between occupied Lewis-type (bond or lone pair) NBO orbitals and formally unoccupied (antibond or Rydeberg) non-Lewis NBO orbital corresponds to a stabilizing donor–acceptor interaction. NBO analysis has been performed on the BHMBC molecule at the DFT/B3LYP/6-311G(d,p) level in order to elucidate, the intra-molecular hybridization and delocalization of electron density within the molecule. The charge transfer within the molecule is more in $\pi \rightarrow \pi^*$ transition. This study reveals the energy transfer during intra-molecular interactions. Transition between πC_1-C_6 and $\pi^* C_2-C_3$, $\pi^* C_4-C_5$ bonds have the energy 18.89 and 20.97 kJ/mol respectively. The occupancy of π bonds are lesser than σ bonds which leads more delocalization. The non-bonding atom n_2O_{10} and O_{36} have 1.86, 1.85 eV as electron density, which transfer maximum energy of 30.27 and 30.36 kJ/mol to the $\pi^* C_1-C_6$, C27—C29 (0.38 eV) bond. From the NBO study, we state that the atom having lone pair of electrons transfer higher energy to its acceptors. The $E(2)$ values and types of the transition are shown in Table S3.

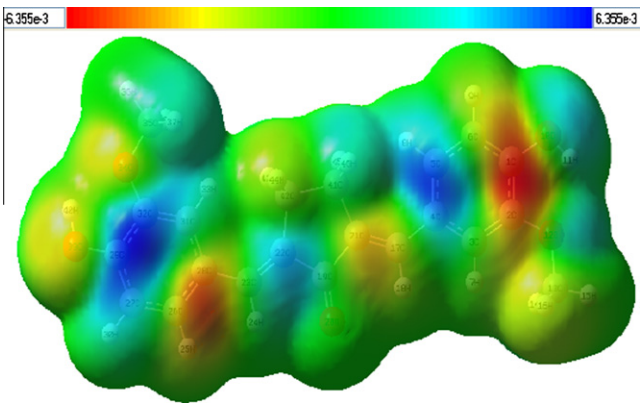

Fig. 5. Molecular electrostatic potential map calculated at B3LYP/6-311G(d,p) level.

9. HOMO–LUMO analysis

Highest occupied molecular orbital (HOMO) and lowest unoccupied molecular orbital (LUMO) are very important parameters for quantum chemistry. We can determine the way in which the molecule interacts with other species; hence, they are called the frontier orbitals. HOMO, which can be thought the outermost orbital containing electrons, tends to give these electrons such as an electron donor. On the other hand; LUMO can be thought the innermost orbital containing free places to accept electrons [54]. The HOMO and LUMO energy calculated by B3LYP/6-311G(d,p) method are mentioned in Table. S4. This electronic transition absorption corresponds to the transition from the ground to the first excited state and is mainly described by an electron excitation from HOMO to LUMO. In the present study, the C=C, O—CH_3 and C—O bond have highest occupied molecular orbital and the LUMO prevails over the C—C bond in BHMBC. The atomic compositions of the frontier molecular orbital are shown in Fig. S4.

10. Molecular electrostatic potential (MEP)

MEP is related to the electronic density and is a very useful descriptor in understanding sites for electrophilic and nucleophilic reactions as well as hydrogen bonding interactions [55,56]. The electrostatic potential $V(r)$ is also well suited for analyzing processes based on the "recognition" of one molecule by another, as in drug–receptor, and enzyme–substrate interactions, because it is through their potentials that the two species first "see" each other [57,58]. To predict reactive sites of electrophilic and nucleophilic attacks for the investigated molecule, MEP at the B3LYP/6-311G(d,p) optimized geometry was calculated. The negative (red[1] and yellow) regions of MEP were related to electrophilic reactivity and the positive (blue) regions to nucleophilic reactivity (Fig. 5). The negative region is localized on the oxygen atoms and the positive region is localized on the hydrogen atom. These results provide information concerning the region where the compound can interact intermolecularly and bond metallically. Therefore, Fig. 5 confirms the non-existence of inter-molecular interactions within the molecule.

11. Conclusion

A complete vibrational and molecular structure analysis has been performed based on the quantum mechanical approach by DFT (B3LYP) calculations. NBO reflects the charge transfer within the molecule. HOMO and LUMO orbitals have been visualized and the band gap energy is also calculated. The UV spectrum was

[1] For interpretation of color in Figs. 1, 2, and 5, the reader is referred to the web version of this article.

measured in methanol solution. ^{13}C NMR and ^{1}H NMR chemical shifts calculations of the BHMBC molecule were carried out by using B3LYP functional with 6-311G(d,p) basis set and the results coincides well with the experimental ^{13}C NMR and ^{1}H NMR. Moreover, molecular electrostatic potential were performed by the DFT methods and the infrared and Raman intensities were also been reported.

Appendix A. Supplementary material

Supplementary data associated with this article can be found, in the online version, at doi:10.1016/j.molstruc.2011.02.039.

References

[1] R.C. Srimal, B.N. Dhawan, J. Pharm. Pharmacol. 25 (1972) 447.
[2] O.P. Sharma, Biochem. Pharmacol. 25 (1976) 1811.
[3] S.C. Sharma, H. Mukhtar, S.K. Sharma, M. Krishna, Biochem. Pharmacol. 21 (1972) 1210.
[4] A. Mukopadhyay, N. Basu, N. Ghatak, P.K. Gujral, Agents Actions 12 (1982) 508.
[5] T. Kosuge, H. Ishida, H. Yamazaki, Chem. Pharm. Bull. (Tokyo) 33 (1985) 1499.
[6] H.H. Tonnesen, Ph.D. Thesis, Institute of Pharmacy, University of Oslo, Norway, 1986.
[7] J. Deli, T. Lorand, D. Szabo, A. Foldesi, Pharmazie 39 (1984) 539.
[8] G.K. Kaushal, Polymer 36 (1995) 1903.
[9] A.G. Griffin, J.F. Johnson, Liquid Crystals and Ordered Fluids, New York, Plenum Press, 1984.
[10] A. Blumstein, Polymeric Liquid Crystals, New York, Plenum Press, 1985.
[11] L.L. Chapoy, Recent Advances in Liquid Crystalline Polymers, London, Elsevier, 1986.
[12] J. Kawamata, K. Inove, T. Inabe, M. Kiguchi, M. Kato, Y. Taniguchi, Chem. Phys. Lett. 249 (1996) 29.
[13] M. Ogawa, Y. Ishii, T. Nakno, S. Irifune, Jpn. Kohai Tokyo. Chem. Abstr. 63 (1988) 238034.
[14] V.D. John, G. Kuttan, K. Krishnankutty, J. Exp. Clin. Cancer. Res. 21 (2002) 219.
[15] L. Shen, H.F. Ji, Spectrochim. Acta 67A (2007) 619.
[16] V. Galasso, B. Kova, A. Modelli, M.F. Ottaviani, F. Pichierri, J. Phys. Chem. 112A (2008) 2331.
[17] Matthew A. Addicoat, Gregory F. Metha, Tak W. Kee, J. Comput. Chem. 20 (2010), doi:10.1002/jcc.21631.
[18] R. Benassi, E. Ferrari, S. Lazzari, F. Spagnolo, M. Saladini, J. Mol. Struct. 892 (2008) 168.
[19] E. Benassi, F. Spagnolo, J. Sol. Chem 39 (2010) 11.
[20] P. Sakthivel, P. Kannan, Polym. Int. 54 (2005) 1490.
[21] Gaussian 03 program, Gaussian Inc., Walling ford CT, 2004.
[22] H.B. Schlegel, J. Comput. Chem. 3 (1982) 214.
[23] D. Michalska, Raint Program, Wroclaw University of Technology, 2003.
[24] D. Michalska, R. Wysokinski, Chem. Phys. Lett. 403 (2005) 211.
[25] J. Baker, A.A. Jarzecki, P. Pulay, J. Phys. Chem. 102A (1998) 1412.
[26] P. Pulay, J. Baker, K. Wolinski. 2013 Green Arc Road, Suite A, Fayettevile, AR72703, USA.
[27] R.J. Butcher, J.P. Jasinski, B. Narayana, B.K. Sarojini, S. Bindya, H.S. Yathirajan, Acta Cryst. E 63 (2007) 3270.
[28] P. Pulay, G. Fogarasi, G. Pongor, J.E. Boggs, A. Vargha, J. Am. Chem. Soc. 105 (1983) 7037.
[29] A.P. Scott, L. Radom, J. Phys. Chem. 100 (1996) 16502.
[30] D. Sajan, H. Joe, V.S. Jayakumar, J. Zaleski, J. Mol. Struct. 785 (2006) 43.
[31] D. Michalska, D.C. Bienko, A.J.A. Bienko, Z. Latajka, J. Phys. Chem. 100 (1996) 17786.
[32] G. Varsanyi, Assignments for Vibrational Spectra of Seven Hundred Benzene Derivatives, vol. 1–2, Academiai Kiado, Budapest, 1973.
[33] B. Stuart, Infrared Spectroscopy: Fundamentals and Applications, John Wiley & Sons Ltd., 2008.
[34] D.l. Pavia, G.M. Lampman, G.S. Kriz, Physics, third ed., in: J. Vondeling (Ed.), Introduction to Spectroscopy: A Guide for Student of Organic Chemistry, vol. 579, Thomson Learning, 2001.
[35] N.P.G. Roeges, A Guide to the Complete Interpretation of Infrared Spectra of Organic Structures, Wiley, New York, 1994.
[36] K.R. Ambujakshan, V.S. Madhavan, H.T. Varghese, C.Y. Panicker, O. Temiz-Arpaci, B. Tekiner-Gulbas, I. Yildiz, Spectrochim. Acta 69A (2008) 782.
[37] J. Karpagam, N. Sundaraganesan, S. Sebastian, S. Manoharan, M. Kurt, J. Raman Spectrosc. 41 (2010) 53.
[38] I. Sidir, Y.G. Sidir, M. Kumalar, E. Tasal, J. Mol. Struct. 964 (2010) 134.
[39] J. Swaminathan, M. Ramalingam, V. Sethuraman, N. Sundaraganesan, S. Sebastian, M. Kurt, Spectrochim. Acta 75A (2010) 183.
[40] N.P.G. Roges, A Guide to the Complete Interpretation of Infrared Spectra of Organic Structures, Wiley, New York, 1994.
[41] N.B. Colthup, L.H. Daly, S.E. Wiberly, Introduction to Infrared and Raman Spectroscopy, third ed., Academic press, Boston, 1990.
[42] S. Sebastian, N. Sundaraganesan, Spectrochim. Acta 75A (2010) 941.
[43] T. Shimanouchi, Y. Kakiuti, I. Gamo, J. Chem. Phys. 25 (1956) 1245.
[44] N.P. Sing, R.A. Yadav, Ind. J. Phys. B 75 (2001) 347.
[45] V. Krishnakumar, R. John Xavier, Spectrochim. Acta 61A (2005) 253.
[46] D.A. Prystupa, A. Anderson, B.H. Torrie, J. Raman Spectrosc. 25 (1994) 175.
[47] R.K. Yadav, N.P. Singh, R.A. Yadav, Ind. J. Phys. B 77 (2003) 419.
[48] D.N. Sathyanarayana, Vibrational Spectroscopy, Theory and Applications, New Age International Publishers, New Delhi, 2004.
[49] M. Karabacak, M. Cinar, S. Ernec, M. Kurt, J. Raman Spectrosc. 41 (2010) 98.
[50] M.J. Frisch, G.W. Trucks, H.B. Schlegel, G.E. Scuseria, M.A. Robb, J.R. Cheeseman, G. Scalmani, V. Barone, B. Mennucci, G.A. Petersson, H. Nakatsuji, M. Caricato, X. Li, H.P. Hratchian, A.F. Izmaylov, J. Bloino, G. Zheng, J.L. Sonnenberg, M. Hada, M. Ehara, K. Toyota, R. Fukuda, J. Hasegawa, M. Ishida, T. Nakajima, Y. Honda, O. Kitao, H. Nakai, T. Vreven, J.A. Montgomery, Jr., J.E. Peralta, F. Ogliaro, M. Bearpark, J.J. Heyd, E. Brothers, K.N. Kudin, V.N. Staroverov, R. Kobayashi, J. Normand, K. Raghavachari, A. Rendell, J.C. Burant, S.S. Iyengar, J. Tomasi, M. Cossi, N. Rega, J.M. Millam, M. Klene, J.E. Knox, J.B. Cross, V. Bakken, C. Adamo, J. Jaramillo, R. Gomperts, R.E. Stratmann, O. Yazyev, A.J. Austin, R. Cammi, C. Pomelli, J.W. Ochterski, R.L. Martin, K. Morokuma, V.G. Zakrzewski, G.A. Voth, P. Salvador, J.J. Dannenberg, S. Dapprich, A.D. Daniels, O. Farkas, J.B. Foresman, J.V. Ortiz, J. Cioslowski, D.J. Fox, Gaussian, Inc. Gaussian 09, Revision A.02, Wallingford CT, 2009.
[51] M. Szafran, A. Komasa, E.B. Adamska, J. Mol. Struct. 827 (2007) 101.
[52] C. James, A. Amal Raj, R. Rehunathan, V.S. Jayakumar, I.H. Joe, J. Raman Spectrosc. 37 (2006) 1381.
[53] L. Jun-na, C. Zhi-rang, Y. Shen-fang, J. Zhejiag. Univ. Sci. 6B (2005) 584.
[54] G. Gece, Corros. Sci. 50 (2008) 2981.
[55] E. Scrocco, J. Tomasi, Adv. Quantum Chem. 11 (1978) 115.
[56] E.J. Luque, J.M. Lopez, M. Orozco, Theor. Chem. Acc. 103 (2000) 343.
[57] P. Politzer, P.R. Laurence, K. Jayasuriya, J. Environ. Health Perspect. 61 (1985) 191.
[58] E. Scrocco, J. Tomasi, Top. Curr. Chem. 7 (1973) 95.